

# ANALYSIS OF HYGROTHERMAL EFFECTS ON THE COMPRESSIVE STRENGTH OF CFRP LAMINATES

C. Soutis

Aerospace Engineering, The University of Sheffield  
Mappin Street, Sheffield, S1 3JD, UK  
[c.soutis@sheffield.ac.uk](mailto:c.soutis@sheffield.ac.uk)

## ABSTRACT

The objective of this paper is to analytically predict the compressive and in-plane shear response of the T800/924C carbon fibre-epoxy composite system (currently available for aerospace structural applications) in hot-wet environments. The weight gains, maximum moisture contents and diffusion coefficients of unidirectional and various multidirectional laminates immersed in boiling water (accelerated ageing) were measured in earlier work and briefly reported here. Data is also presented on the effects of moisture and temperature on the uniaxial compressive strength/failure mode of unidirectional laminates and multidirectional plates with an open hole. It is observed that the failure in the hot-wet specimens always occurs as a result of out-of-plane microbuckling of the  $0^\circ$  plies. This is attributed to the reduction in matrix strength properties and weakening of the ply interface arising from elevated temperatures and environmental conditioning. Test results are compared to theoretical predictions made by the Budiansky fibre microbuckling model and the Soutis-Fleck cohesive zone model for the notched compressive strength.

## 1. INTRODUCTION

Fibre reinforced plastics are increasingly being used in the manufacture of civil aircraft structural components (Boeing 787, Airbus A380) and in order to certify these components for service use it is important to examine their mechanical behaviour under a range of environmental conditions. It is known that hot and humid environments can degrade some aspects of the material performance in particular the compressive strength [1-6]. Water absorption by the epoxy resin leads to a reduction in the glass transition temperature and to a softening of the resin with a loss of stiffness and strength, which causes fibre microbuckling and premature laminate failure [5, 6]. The degradation increases as the conditions become more severe. The quantity of water absorbed by a laminate is therefore of considerable importance, in particular to the designer when setting design limits for structures operating in humid environments. The aim of the present work is to analytically estimate the water absorption effect (exposure to boiled water, accelerated ageing) on the compressive strength of unidirectional and multidirectional T800/924C carbon fibre-epoxy

laminates and compare these results to experimental data obtained in earlier studies by the author and co-workers [5].

## **2. EXPERIMENTAL PROCEDURE**

### **2.1 Materials and test specimens**

Laminates measuring 1000 mm x 300 mm were manufactured from T800/924C carbon fibre-epoxy prepreg supplied by Hexcel Composites Ltd; the composite contained approximately 65% by volume fibres. The laminates were consolidated and cured in an autoclave at a temperature of 170°C for 1 h and subsequently post-cured for 4 h at 190°C. Three different lay-ups were produced: a 16-ply unidirectional (UD) and two 24-ply multidirectional (MD) laminates having a stacking sequence of  $[(\pm 45/0_2)_3]_s$  and  $[(90_2/0_2)_3]_s$ . Immediately after manufacture, the laminates were cut into specimens measuring 110 mm x 10 mm for the unidirectional and 240 mm x 50 mm for the multidirectional, and stored in a desiccator to minimise moisture absorption prior to testing or environmental conditioning. A 5 mm diameter hole was drilled at the centre of each multidirectional specimen using a tungsten carbide bit [5].

### **2.2 Environmental exposure**

In earlier work [5] the composite specimens were immersed in boiling water so the equilibrium level was reached in a period of few weeks (accelerated ageing); in order to measure moisture content data normally requires exposure times of over six months, even for relatively thin laminates of say 1 mm thick [5,7]. During the conditioning the specimens were periodically removed from the environment and weighed using an electronic balance accurate to  $\pm 0.0001$  g. Their weight gain, expressed as a percentage of their dry weight, was plotted against square root time ( $\sqrt{\text{Days}}$ ) in order to measure the equilibrium level  $M_\infty$ , i.e. the maximum amount of moisture that can be absorbed by a laminate at a given humidity. The slope of the linear part was used subsequently in the calculation of the diffusion coefficient  $D_\infty$ . After the maximum moisture content reached the specimens were removed and weighed once more and stored in a desiccator before being mechanically tested. Those specimens to be tested in the dry condition were loaded to failure within about 10 minutes of being removed from the desiccator and although it is acknowledged that some moisture absorption might have occurred, it is assumed that the moisture content in these specimens is negligible [1].

### **2.3 Apparatus and mechanical tests**

#### **2.3.1 Unidirectional Specimens**

Compression tests on the unidirectional specimens were performed following the procedures outlined in CRAG tests methods [8], using a modified Celanese test jig [3-5] at a constant compression rate of  $0.017 \text{ mm s}^{-1}$  on a screw-driven machine of load capacity 50 kN. The conventional serrated grip faces of the Celanese were replaced by spark eroded

inserts (20 Ra) to eliminate adhesively bonded tabs on the specimen ends [5]; by having no tabs the entire surface of the specimen was exposed for water absorption. To measure the compressive strength as a function of temperature and humidity, two extra inspection ports were drilled on the Celanese alignment sleeve, so a hot-air blower and a steam pipe could be attached. Symmetric airflow was achieved and the specimen was heated evenly. The temperature and humidity of the environment were monitored regularly by a thermocouple and a Testoterm hygrometer. It took less than 5 min to reach 100°C and the environmental conditioning chamber was capable of maintaining the temperature to within 3°C. The specimens were allowed to ‘soak’ for about 10 min before being tested. At least five tests were carried out per test condition, hot-dry (20°C-100°C) and hot-wet (20°C-100°C, 95% RH). Strain gauges were used on both faces of all specimens to be tested in hot-dry conditions to measure axial strain and monitor the degree of Euler bending.

### ***2.3.2 Multidirectional Specimens***

The multidirectional notched specimens were tested under the same hot-dry and hot-wet conditions as the unidirectional specimens using a home-made environmental chamber in a servo-hydraulic test machine at a loading rate of 1 kN s<sup>-1</sup>. The specimens were untabbed straight-sided and were loaded by shear action by means of wedge grips with a spark eroded surface finishing [5]. They were of gauge section 120 mm x 50 mm, and were tested by using an anti-buckling device to prevent buckling (Euler bending) during the test. The anti-buckling device increases the flexural stiffness of the composite plate but carries no load. Considerations of importance throughout the compressive test procedure were alignment of the specimen in the grips and proper attachment of the anti-buckling device to the specimen. Full details on the experimental technique have been documented previously by Soutis [9-11].

## **3. TEST RESULTS AND DISCUSSION**

The experimental results consist of moisture absorption measurements, and compressive strength/stiffness data for unidirectional and multidirectional notched laminates. The shear properties of the T800/924C system (measured by using the Iosipescu specimen) are also presented in order to understand how shear properties affect the compressive behaviour.

### **3.1 Moisture absorption**

In a carbon fibre reinforced epoxy resin the resin absorbs moisture while the fibres do not absorb. Most of the evidence in the literature suggests that water is absorbed by a bulk diffusion mechanism in the resin and for flat plates the rate of moisture absorption  $\partial M / \partial t$  through the thickness direction ( $z$ ) can be described by Fick’s second law:

$$\frac{\partial M}{\partial t} = D \frac{\partial^2 M}{\partial z^2} \quad (1)$$

where  $D$  is the diffusion coefficient. It should be remembered that the two main characteristics of Fickian behaviour are: **i)** the absorption curve should be linear initially and **ii)** the moisture content should reach a saturation level ( $M_\infty$ ) at large values of time. The analytical solution of equation (1) yields the amount of moisture uptake, which varies with time as [12]

$$M(t) = M_o + (M_\infty - M_o) \frac{4}{h} \sqrt{\frac{Dt}{\pi}} \quad (2)$$

where  $M_o$  is the initial amount of moisture in the solid,  $M_\infty$  is the final amount at equilibrium and  $h$  is the laminate thickness. From equation (2) it is clear why the initial part of the plot of  $M(t)$  versus the square root of time should be a straight line. The diffusivity can then be determined by using the value of  $M$  for two different values of time:

$$D = \pi \left( \frac{h}{4(M_\infty - M_o)} \right)^2 \left( \frac{M(t_2) - M(t_1)}{\sqrt{t_2} - \sqrt{t_1}} \right)^2 \quad (3)$$

Eqn (3) is often considered with  $M_o=0$ . Using Eqn (3) and the slope of moisture content data described in section 2.2 the diffusivity for the unidirectional and  $[(\pm 45/0_2)_3]_s$  multidirectional laminate were obtained and presented in Table 1.

**Table 1.** Coefficient of moisture diffusion for T800/924C laminates

Diffusivity mm <sup>2</sup> /s	$[0_8]_s$	$[(\pm 45/0_2)_3]_s$
$D$	$1.2 \times 10^{-6}$	$1.1 \times 10^{-6}$
$D_\infty$	$8.42 \times 10^{-7}$	$9.3 \times 10^{-7}$

The slope  $M / \sqrt{t}$  was obtained in [5] from using the complete specimen (finite plate) and therefore includes moisture diffused through all six surfaces. This gives a greater slope than would have been obtained for an infinite plane sheet as moisture had diffused through six sides instead of two. To give a better estimate of the true one-dimensional diffusivity coefficient  $D_\infty$  a correction factor given by Shen and Springer [13] was used. From Table 1 it can be seen that the diffusivity of the multidirectional laminate is about 10% higher than that of the unidirectional laminate, probably due to more entrances available for the water to diffuse through the plate and due to larger interfacial absorption of the 45° plies [14]. The diffusion coefficient and the equilibrium moisture content ( $M_\infty = 1.42\%$ ) were used by Soutis *et al.* [5] with a computer program developed by Copley [7] to estimate the through thickness moisture distribution and concluded that although Fickian diffusion did not exactly model the actual diffusion, it was sufficiently accurate for the cases examined.

## 3.2 Compressive strength of unidirectional laminates

### 3.2.1 Strength data and failure modes

The effect of temperature and environmental conditioning on the compressive strength/stiffness of the T800/924C unidirectional laminate is presented in Table 2; shear strength properties are also given. The values in brackets are estimated by the Budiansky fibre microbuckling model [15], presented and discussed in section 4.1. It can be seen that moisture and high temperature has a marked influence on the composite's compressive behaviour. At operating temperature of 100°C-dry the strength has been reduced by more than 30% and the failure strain has dropped from 0.96% to 0.73% (approximately 24% reduction). This is because the stiffness of the epoxy resin is reduced substantially with increasing temperature; the shear modulus has been reduced by almost 20%, Table 2. In uniaxial compression reduction in matrix modulus means reduced support for the fibres, which promotes premature failure of the composite by out-of-plane fibre microbuckling. The compressive strength is further reduced (by 54%) when the laminate contains 1.4% by weight moisture and tested at 100°C and 95% RH. It can be seen from the results shown in Table 2 that the compressive strength ( $\sigma_c$ ) is approximately 20% of the elastic shear modulus; remember that Rosen's analysis of fibre buckling predicts that  $\sigma_c$  is equal to the shear modulus. This suggests that a plastic-buckling analysis is required in order to estimate strength more accurately. The results quoted in Table 2 are based on the average of five specimens tested at each environmental condition; the coefficient of variation is less than 5%. For the specimens tested in hot-wet environment there are no experimental data for the axial Young's modulus and shear strength and stiffness properties since bonding of electric strain gauges in such specimens was found difficult, however, estimated values are given, see section 4.

Compressive failure of the room temperature unidirectional specimens was sudden and occurred mainly within the specimen gauge length. In-plane fibre microbuckling (fibres bend and rotate in the 1-2 plane) was considered as the critical damage mechanism, which causes the catastrophic fracture, Fig.1. Longitudinal splits and fibre/matrix debonding do not occur gradually but take place suddenly and concurrently with the final failure. The specimens generally fail along a 15°(= $\beta$ ) line from the transverse axis [4, 5]. In the case of specimens tested at hot-wet conditions damage occurred in the middle of the specimen and grew almost perpendicular to the loading axis. Subsequent examination by scanning electron microscopy revealed that the fibres underwent out-of-plane (1-3 plane) microbuckling. The strain at which this failure mode initiates is reduced with increasing temperature and at 100°C is only 75% of the strain required to initiate in-plane microbuckling. Thus, any weakening of the matrix or fibre/matrix interface arising from elevated temperatures and environmental conditioning increases the probability of out-of-plane buckling of the fibres which results in degraded compressive strength.

**Table 2.** Measured compressive strength properties of T800/924C unidirectional laminates

Test Temperature °C	Compressive Strength MPa	Young's Modulus* GPa	Shear Strength MPa	Shear Yield Stress MPa	Shear Modulus GPa
20-dry	1415 (1411)	160	110	40	6.0
20-wet	1060 (1040)	-	(89)	(29.5)	(5.4)
50-dry	1230 (1235)	155	105	35	5.8
50-wet	930 (917)	-	(78)	(26)	(5.4)
80-dry	1137 (1129)	149	98	32	5.4
80-wet	828 (829)	-	(69)	(23)	(4.9)
100-dry	973 (953)	136	90	28	4.9
100-wet	654 (653)	-	(54)	(18.5)	(4.5)

\*Secant modulus measured at 0.25% axial strain; ( ) estimated values by Budiansky's model [15] and the measured UD compressive or shear strength properties. Initial fibre misalignment,  $\phi_0=1.75^\circ$ , kink band inclination angle,  $\beta=15^\circ$ .

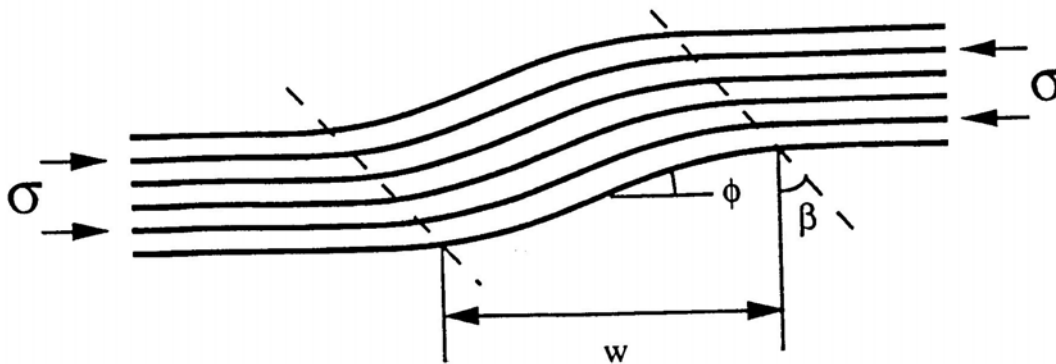


Figure 1. A schematic showing the geometry of the fibre microbuckling failure mode.

### 3.3 Compressive strength of multidirectional laminates

#### 3.3.1 Strength data and failure modes

Compressive strength results for two multidirectional laminates with a 5 mm hole ( $d/W=0.1$ ) tested at various environmental conditions [5] are summarised in Table 3. Strength values are based on the cross-sectional area of the test piece. It is clear that the compressive strength of the  $[(\pm 45, 0_2)_3]_s$  laminate is reduced by more than 40% when the

specimen contains 1.42% moisture and is tested at 100°C-wet conditions (the room temperature unnotched strength is 812 MPa). The scatter in strength is less than 10% and all specimens failed from the hole in a direction almost perpendicular to the loading axis.

**Table.3** Compressive strength results for T800/924C laminates with a 5mm hole.

Test temp °C	OHC Strength MPa [(± 45, 0 <sub>2</sub> ) <sub>3</sub> ] <sub>s</sub>	Predicted OHC Strength* MPa [(± 45, 0 <sub>2</sub> ) <sub>3</sub> ] <sub>s</sub>	OHC Strength MPa [(90 <sub>2</sub> , 0 <sub>2</sub> ) <sub>3</sub> ] <sub>s</sub>	Predicted OHC Strength* MPa [(90 <sub>2</sub> , 0 <sub>2</sub> ) <sub>3</sub> ] <sub>s</sub>
20-Dry	451.75	342.0	351.65	290.9
20-Wet	402.00	293.6	-	232.0
50-Dry	421.50	309.6	324.67	259.7
50-Wet	357.50	259.0	-	211.2
80-Dry	371.50	293.9	291.37	244.4
80-Wet	325.00	241.2	-	195.1
100-Dry	-	265.5	-	217.5
100-Wet	282.00	208.3	-	167.6

\* Longitudinal UD compressive strength, shear yield strength (Table 2) and  $G_C(\tau_y)$  are the input data in [16, 17] for the predicted OHC results

Penetrant-enhanced X-ray radiography and scanning electron microscopy revealed that failure was by microbuckling of the 0° plies, and was accompanied by delamination between the off-axis and 0° layers, and by plastic deformation in the off-axis plies.

## 4. THEORETICAL STRENGTH PREDICTIONS

### 4.1 Unnotched compressive strength

The compressive strength of long, aligned carbon fibre-reinforced plastics (CFRP) is significantly lower (30%-40%) than the tensile strength of the material due to kink-band formation introduced by fibre instability (microbuckling). For an elastic-perfectly plastic body Budiansky [15] showed that

$$\sigma = \frac{\tau_y \left[ 1 + \left( \frac{\sigma_{T_y}}{\tau_y} \right)^2 \tan^2 \beta \right]^{\frac{1}{2}}}{\phi_0 + \phi} \quad (4)$$

where  $\tau_y$  and  $\sigma_{Ty}$  are the in-plane shear and transverse yield stresses of the composite, respectively.  $\phi_0$  is the assumed fibre misalignment angle in the kink-band,  $\phi$  is the additional fibre rotation in the kink-band under a remote stress  $\sigma$ , and  $\beta$  is the band orientation angle, as shown in Figure 1. The critical stress  $\sigma = \sigma_c$  is achieved at  $\phi = 0$  in equation (4). Using equation (4) with the experimental shear strength data for the T800/924C system the UD compressive strength is obtained, Table 2; it can be seen that agreement is very good (less than 3% difference). Also, for the hot-wet specimens where shear data weren't available equation (4) is employed with the measured UD strength to obtain these values, see Table 2. Once the failure stress of the 0°-ply is known, the compressive strength of any multidirectional (MD) 0°-dominated lay-up,  $\sigma_{un}$ , can be estimated by the laminate plate theory and the maximum stress failure criterion. The room temperature unnotched compressive strength for the  $[(\pm 45, 0_2)_3]_s$  and  $[(90_2/0_2)_3]_s$  laminates based on the maximum stress failure criterion is approximately 812 MPa and 747 MPa, respectively.

## 4.2 Open hole compressive (OHC) strength

The compressive strength of the composite plate is reduced by the presence of fastener holes and access cut-outs. Previous work by Soutis and co-workers [9-11] have found that open holes cause more than 40% reduction in the strength of carbon fibre-epoxy and carbon fibre-PEEK laminates and that damage was initiated by fibre microbuckling in the 0° plies at the edge of the hole. Soutis *et al* [10] compared the damage zone (microbuckling surrounded by delamination) at the edge of the hole to a through-thickness line crack containing cohesive stresses. This equivalent crack is loaded on its faces by a normal traction,  $T$ , which decreases linearly with the crack closing displacement (CCD),  $2v$ . It is assumed that the length of the equivalent crack  $\ell$  represents the length of the microbuckle. When the remote load is increased the equivalent crack grows in length, thus representing microbuckle growth. The evolution of microbuckling is determined by requiring that the total stress intensity factor at the tip of the equivalent crack equals zero. When this condition is satisfied, stresses remain finite everywhere [10]. The model contains two unknown parameters, which can be measured independently or predicted analytically [16]: the unnotched strength  $\sigma_{un}$  and the critical CCD  $v_c$ , which is related to the area  $G_C$  (fracture energy) under the assumed linear traction - crack displacement curve. For a linear softening cohesive zone law the critical strain energy release rate  $G_C$  is given by

$$G_c = 2 \int_0^{v_c} \sigma(v) dv = \sigma_{un} v_c \quad (5)$$

where  $v_c$  is the critical crack closing displacement on the crack traction- crack displacement curve, which is analogous to the crack opening displacement in tension. It is assumed that the fracture energy  $G_C$  represents the total energy per unit projected area dissipated by fibre microbuckling. Of course other damage modes may occur within this process zone like matrix plasticity in the off-axis plies and delamination, but the critical damage mechanism is the fibre kinking or microbuckling. Budiansky [15] in his microbuckling analysis for an



idealised unidirectional lamina related the crack overlap displacement  $2v_c$  explicitly to fibre diameter and fibre volume fraction by [16]:

$$2v_c = w = \frac{\pi d_f}{4} \left( \frac{V_f E_f}{2\tau_y} \right)^n \quad (6)$$

where  $d_f$  is the fibre diameter,  $E_f$  is the fibre elastic modulus and  $\tau_y$  is the in-plane shear yield stress of the composite. For carbon fibre/epoxy system the exponent  $n=1/3$ . Once the CCD and unnotched strength are known the fracture energy associated with fibre microbuckling can be obtained from equation (5) and material data presented in Table 2. For the T800/924C system examined here and room temperature conditions,  $V_f=0.6$ ,  $d_f=5.6\mu\text{m}$ ,  $E_f=267$  GPa and  $\tau_y=40$  MPa, which result to a  $2v_c=56$   $\mu\text{m}$  and hence  $G_C=22.74$   $\text{kJ/m}^2$  ( $K_C=40.8$   $\text{MPa}\sqrt{\text{m}}$ ) for the  $[(\pm 45, 0_2)_3]_s$  laminate. The observed kink-band width  $w$  ( $=2v_c$ ) from several optical micrographs that were obtained from sectioning studies was in the region of 10-12 fibre diameters (56-67  $\mu\text{m}$ ). In Table 3 the experimental open hole compressive strengths for the two T800/924C  $[(\pm 45, 0_2)_3]_s$  and  $[(90_2/0_2)_3]_s$  laminates are presented for different hot-dry and hot-wet conditions and compared to those obtained by the Soutis-Fleck cohesive zone model, which has been implemented in a commercially available computer package [17]. The predicted OHC results are up to 25% lower than the measured values since energy dissipated in the form of matrix cracking and delamination are not included in the fracture model. A smaller difference is observed for the 90/0 lay-up suggesting that the amount of off-axis ply damage is less extensive.

## 5. CONCLUDING REMARKS

Untabbed straight-sided unidirectional and multidirectional specimens were tested following the procedures outlined in CRAG test methods [8]. The faces of the grip inserts of the test apparatus were spark-eroded to produce a surface finish of approximately 20 Ra. No damage to the surface plies was observed in specimens with uniform thickness and acceptable failure modes and location of failure were obtained. The diffusion coefficient and the equilibrium moisture content were measured; it was found that although Fickian diffusion did not exactly model the actual moisture absorption, it was sufficiently accurate for the cases examined [5]. The strength properties of specimens tested in hot-wet conditions were substantially reduced and the final failure always occurred due to out-of-plane fibre microbuckling. This is attributed to the reduction in matrix strength properties and weakening of the ply interface with increasing temperature and environmental conditioning. Thus, in compression the matrix and interface play a key role in providing side support to the fibres and consequently resistance to fibre buckling. The cohesive zone fracture model by Soutis-Fleck [10, 11] was successfully applied to predict the open hole compressive strength for two different multidirectional orthotropic laminates tested in hot-dry and hot-wet environments. The model contains two unknown parameters, which can be measured independently or predicted analytically [16]: the unnotched strength  $\sigma_{un}$  and the critical CCD  $v_c$ , which is related to the area  $G_C$  (fracture energy associated with fibre

microbuckling) under the assumed linear traction-crack displacement curve. Other damage modes may occur within this process zone such as matrix plasticity in the off-axis plies and delamination, but the critical damage mechanism is the fibre kinking or microbuckling.

## 6. REFERENCES

1. Potter, R.T. and Purslow, D. The environmental degradation of notched CFRP in compression, *Composites*, 1983, **14**(3), 206-225.
2. Barker, A.J. and Balasundaram, V. Compression testing of carbon fibre-reinforced plastics exposed to humid environments, *Composites*, 1987, **18**(3), 217-226.
3. Soutis, C. and Turkmen, D. Influence of shear properties and fibre imperfections on the compressive behaviour of GFRP laminates. *Appl. Comp. Materials*, 1995, **6**(2), 327-342.
4. Soutis, C. and Turkmen, D. Moisture diffusion in T800/924C carbon fibre-epoxy laminates. *Adv. Comp. Lett.*, 1995, **4**(4), 115-120.
5. Soutis, C. and Turkmen, D. Moisture and temperature effects on the compressive failure of CFRP unidirectional laminates. *J. Composite Materials*, 1997, **31**(8), 832-849.
6. Browning, C.E., Husman, C.E. and Whitney, J.M. Moisture effects in epoxy matrix composites, *AFML-TR-77-41* (1977).
7. Copley, S.M. A computer program to model moisture diffusion and its application to accelerated ageing of composites, *Royal Aircraft Establishment (RAE)*, TR-82010 (1982).
8. Curtis, P.A. CRAG test methods for the measurement of the engineering properties of fibre-reinforced plastics, *RAE*, TR- 85099 (1985).
9. Soutis, C. and Fleck, N.A. Static compression failure in carbon fibre T800/924C composite plate with an open hole, *J. Comp. Mater.*, 1990, **24**, 538-556.
10. Soutis, C., Fleck, N.A. and Smith, P.A.. "Failure prediction technique for compression loaded carbon fibre-epoxy laminate with an open hole". *J. Comp. Mat.*, 1991, **25** 1476-98.
11. Soutis, C., Curtis, P.T. and Fleck, N.A. "Compressive failure of notched carbon fibre composites". *Proc. R. Soc. London A*, 1993, **440**, 241-256.
12. De Wilde, W.P. and Frolkovic, P. The modelling of moisture absorption in epoxies: effects at boundaries, *Composites*, 1994, **25**(2), 119-127.
13. Shen, C. and Springer, G.S. Moisture absorption and desorption of composite materials, *J. Comp. Mater.*, 1976, **10**, 2-20.
14. Naeem, M. The resistance of glass reinforced thermosetting polymers to thermohumid conditions, *PhD. Thesis*, Loughborough University of Technology (1995).
15. Budiansky, B. Micromechanics. *Computers and Structures*, 1983; **16**(1): 3-12.
16. Soutis, C. and Curtis, P.T. A method for predicting the fracture toughness of CFRP laminates failing by fibre microbuckling. *Composites A*, 2000; **31**(7): 733-740.
17. Laminate Analysis Program (LAP), Composite Materials Design Tool, Version 4, 2002 by Anaglyph Ltd.